

## A Fast Line-by-Line Method for Atmospheric Absorption Computations: The Automatized Atmospheric Absorption Atlas

N. A. SCOTT AND A. CHEDIN

Laboratoire de Météorologie Dynamique du C.N.R.S., École Polytechnique, 91128 Palaiseau Cedex, France

(Manuscript received 3 December 1980, in final form 27 March 1981)

### ABSTRACT

A computationally fast line-by-line method for the determination of atmospheric absorption is described. This method is based on the creation of an Automatized Atmospheric Absorption Atlas (4A) covering all possible plausible atmospheric conditions (temperature, mixing ratios of absorbing gases, zenith angle). It is applied to synthetic computations of atmospheric transmittances and radiant energies associated with three types of satellite observations: radiometric measurements made by HIRS/2 (High-Resolution Infrared Sounder) on TIROS-N; infrared images taken from the geostationary satellite METEOSAT; interferometric experiment IRIS (Infrared Interferometer Spectrometer) on VOYAGER (NASA's mission to Jupiter, Saturn and possibly Uranus). For all three experiments, comparisons were made with real observations and are presented associated with radiosonde data for the first. Concerning computation times, a gain of a factor varying between 15 and 40 is obtained when using the 4A line-by-line method rather than a standard line-by-line method.

### 1. Introduction

The global coverage associated with satellite experiments makes retrievals of atmospheric parameters from radiometric measurements extremely repetitive and leads to the necessity of using efficient models for determining transmittances and radiant energies. The governing equation for the radiant energy reaching the top of a plane-parallel stratified atmosphere overlying a black surface at pressure  $P_G$  is

$$I_j = B(T(P_G), \nu_j) \tau_j(P_G, 0) + \int_{P_G}^0 B(T(P), \nu_j) \frac{\partial \tau_j(P, 0)}{\partial \ln P} \partial \ln P,$$

where  $B(T, \nu)$  is the Planck's spectral radiance at temperature  $T$  and at frequency  $\nu$ . In this equation, convolution by the instrument function has been omitted for the sake of simplicity. Monochromatic transmittance  $\tau_j(P, 0)$  between the top of the atmosphere and the pressure level  $P$  may be formulated as

$$\tau_j(P, 0) = \exp \left\{ - \int_P^0 \mathcal{K}[\nu_j, T(P)] dP \right\},$$

where  $\mathcal{K}[\nu_j, T(P)]$  may be expressed by the sum of the contributions to the absorption coefficient of all the lines of the atmospheric spectrum. The most accurate method for deriving atmospheric

absorption is by summing the contributions of all the absorption lines of all the absorbing gases in very narrow spectral intervals (generally of the order of magnitude of a line half-width), all along the optical path—this method is known as the line-by-line and layer-by-layer method. Owing to numerous applications to radiative transfer in the earth or in planetary atmospheres, we have found out that this method presents all the required accuracy and flexibility. In particular, it allows atmospheric inhomogeneities to be fully taken into account as well as any instrumental function. Computation times were of the order of several seconds per centimeter (from  $\sim 1$  s  $\text{cm}^{-1}$  to more than 10 s  $\text{cm}^{-1}$  according to the spectral region investigated). This obviously forbids such a method being used for real-time processing of satellite data. This is the reason for which faster algorithms have been recently developed (see, e.g., McMillin and Fleming, 1976; McMillin *et al.* 1979; Fleming and McMillin, 1977; Abel *et al.*, 1978)<sup>1</sup> which apply the line-by-line method to a restricted predetermined set of atmospheric conditions (temperature, humidity, etc.) and then develop a means for extrapolating to other conditions. The accuracy and the stability of such models, developed for a specific satellite experiment

<sup>1</sup> Abel, P. G., W. L. Smith and A. Arking, 1978: An empirical model for atmospheric transmittance functions and its application to the Nimbus 6 HIRS experiment. NOAA Tech. Memo. NESS 99, 32 pp.

(like HIRS/2 on TIROS-N) are related to the number of line-by-line computations from which the unknown coefficients entering the extrapolation procedure are derived. In the abovementioned references, line-by-line transmittance calculations were made for a set of 32 atmospheric profiles, each at five zenith angles. The efficiency of models of that kind could probably be improved by enlarging the sample set whose rather limited size is only due to computation time and expense considerations. Such a limitation would disappear with a faster line-by-line method. Faster line-by-line procedures also are required for the analysis of experimental spectra recorded by high spectral resolution instruments on aircraft, balloons or satellites, like interferometers. This is mainly the case for studies on the stratosphere and on planetary atmospheres for which atmospheric conditions (temperature and/or composition) are not very well known or are unknown and must be constantly varied by often large amounts when adjusting theory to experiment.

The approach used in this paper for obtaining a computationally fast and general line-by-line method consists, at first, in using a standard line-by-line procedure to derive the transmittances, *monochromatically* for the whole of the spectral region of interest, of individual layers of a stratified atmosphere for a large set of plausible atmospheric conditions and, then, in developing a means of reconstituting the transmittance profile for any atmospheric conditions. In the following, this method for computing atmospheric transmittances will be referred to as the Automatized Atmospheric Absorption Atlas or 4A. As an example, the 4A model for the Earth has been designed on the basis of an atmosphere divided into 38 pressure levels ranging from the pressure at the surface to  $\sim 0.05$  mb (see Fig. 1). Comprised between two pressure levels, each layer is given a maximum plausible temperature variation and the transmittances are evaluated for a set of temperatures ranging from the smallest temperature to the largest with a sampling interval  $\Delta T$ . These computations are carried out for a reference mixing-ratio profile for each of the absorbing gases and for a reference zenith angle.

From the 4A data set, which has absorbed most of the long and tedious computations, it is easy to derive the transmittances of the whole atmosphere for any atmospheric conditions. Assuming the same pressure stratification as for the 4A data set, transmittances of each layer of the atmosphere considered are directly obtained from the 4A predetermined set of individual layer transmittances (same pressure; closest temperature) and then multiplied to give the required transmittances between the observation point and any other point in the atmosphere. Modifications of the mixing ratios and zenith angle reference values are simply made

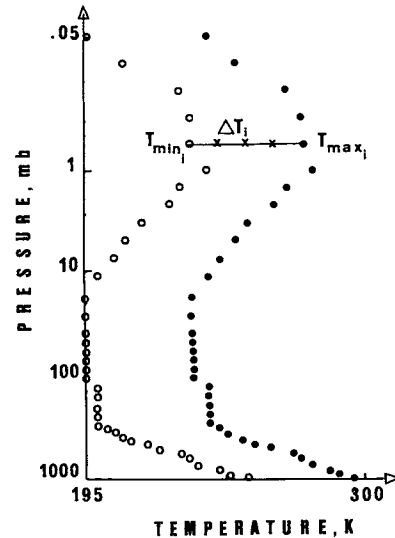


FIG. 1. Temperature modeling and sampling of the Earth atmosphere with the 4A model: the two extreme temperature profiles [cold (open circles), hot (solid circles)] versus logarithm of pressure are shown as well as the temperature sampling of the  $i$ th layer.

by elevating the predetermined transmittances to the correct power. This operation is performed in such a way that it does not require additional computation time.

Errors introduced by the use of the 4A line-by-line method as compared to the standard line-by-line method are essentially due to the differences in temperature between each real layer of the given atmosphere and the corresponding predetermined layer included in the 4A data set. These differences are, at maximum, equal to  $\Delta T/2$ . Interpolation in temperature, which should be made on each frequency point, is avoided since the value of the sampling temperature interval  $\Delta T$  may be adjusted according to the sensitivity of transmittances to temperature. In addition, these errors are sometimes positive and sometimes negative and compensate each other up to a large extent in the final results that are the products of individual layer transmittances.

The 4A line-by-line method has resulted in a decrease of the computation time by at least one order of magnitude. The derivation of the 4A predetermined set of transmittances is developed in Section 2. The 4A line-by-line transmittances computation method is presented in Section 3 and applied in Sections 4 and 5 to three different types of satellite experiments: atmospheric vertical sounder HIRS/2 on TIROS-N, infrared imaging radiometer on METEOSAT, and interferometer IRIS (Infrared Interferometer Spectrometer) on VOYAGER 1 and 2. Section 6 presents additional technical details on storing the 4A data set.

TABLE 1. Percentages of monochromatic transmittances greater than 0.999 or greater than 0.995 in three  $5 \text{ cm}^{-1}$  wide spectral intervals of the  $15 \mu\text{m}$  spectral region, for 8 of the 38 layers of the atmospheric stratification of the 4A model, for a given  $P$ ,  $T$  atmospheric model.

Layer ↓	$\bar{P}$ (mb)	$\bar{T}$ (K)	655–660 $\text{cm}^{-1}$		705–710 $\text{cm}^{-1}$		775–780 $\text{cm}^{-1}$	
			Percent transmittance		Percent transmittance		Percent transmittance	
			>0.999	>0.995	>0.999	>0.995	>0.999	>0.995
1	0.06	224	97	99	99	100	100	100
3	0.2	254	95	97	99	99	100	100
5	0.8	270	85	94	94	98	99	100
8	3	250	49	77	82	92	98	99
12	12	225	8	31	37	72	92	97
17	60	215	0	0	0	0	79	95
24	300	230	0	0	0	0	48	85
37	900	280	0	0	0	0	0	0

## 2. The predetermined set of monochromatic transmittances (Automatized Atmospheric Absorption Atlas or 4A)

We first consider a stratified atmosphere divided into  $N$  pressure levels. To each layer, comprised between two successive pressure levels,  $P_{i-1}$  and  $P_i$ , we associate two temperatures,  $(T_{\min})_i$  and  $(T_{\max})_i$ , which represent the extreme limits of variation of this parameter at the mean pressure  $\frac{1}{2}(P_i + P_{i-1})$  for all observed or plausible atmospheric conditions. In the spectral region of interest, limited by the frequencies  $\nu_a$  and  $\nu_b$ , a standard line-by-line computation is carried out for all the layers and, for each layer, for all the temperatures from  $(T_{\min})_i$  to  $(T_{\max})_i$  with a temperature sampling step  $\Delta T$ . For narrow spectral regions—let's say, a few  $\text{cm}^{-1}$  wide—the step  $\Delta T$  is a constant and is adjusted to the sensitivity of transmittances to temperature in this spectral region. Orders of magnitude are  $5^\circ\text{C}$  for small dependences and  $1^\circ\text{C}$  or less for strong dependences. Large spectral regions (e.g., the HIRS/2 channels) are divided into sub-intervals and the preceding holds for each sub-interval. These standard line-by-line computations are performed in several steps: in the first step, only the absorbing gases whose mixing ratios do not vary with altitude are considered and their contributions to absorption are summed; and in the next steps, the absorbing gases whose mixing ratios vary with altitude are considered successively and their contributions to absorption are stored separately.

Consequently, for each layer and for each of the temperatures sampled for this layer, the line-by-line computation results in as many transmittance vectors (transmittances versus frequency, the frequency step being of the order of magnitude of the line half-width at the mean pressure value associated to the layer) as there are absorbing gases with mixing ratios varying with altitude plus one for the sum of the absorbing gases with a constant

mixing ratio. These standard line-by-line computations are made with a reference zenith angle  $\theta_{\text{ref}}$  and with a reference mixing-ratio profile for each absorbing gas with a variable mixing ratio  $q_{\text{ref}}$ .

The results of these computations constitute the predetermined set of transmittances which is at the basis of the 4A data set. For large spectral intervals and for the frequency step mentioned above, these results may represent a very large volume of data which must be preserved in such a way that any piece of information (i.e., transmittance versus frequency for one layer at one temperature and separately for the various absorbers) can be reached instantaneously. Fortunately, a careful quantitative examination of such data brings into evidence a very large number of data points for which transmittance is very close to 1. This is illustrated by Table 1. For a set of eight layers, representative of the various regions of the atmosphere (Earth), this table gives, for three spectral intervals, ( $5 \text{ cm}^{-1}$  each in the  $15 \mu\text{m}$  region) and for each of the eight layers, the percentage of data points for which the transmittance (cumulated over all the absorbing gases) is either greater or equal to 0.999 or greater or equal to 0.995. From this table, it is interesting to notice that the largest percentages correspond to layers associated with small pressures, themselves corresponding to the smallest frequency steps. This accounts for the greater transparency of the upper atmosphere. The 4A predetermined set of transmittances is made of the data points for which transmittance is less than  $1 - \epsilon$  (under reference conditions  $\theta_{\text{ref}}$ ,  $q_{\text{ref}}$ ),  $\epsilon$  being close to zero. In other words, for each layer at a given temperature and for each of the transmittance vectors considered earlier, all the points in frequency whose contribution to absorption is too small are eliminated and consequently not stored. Marking in frequency of each data point which is effectively stored in the 4A data set is ensured by an integer index—the frequency marker. A quite considerable reduction

of the number of data points which must be stored is then achieved. We have considered, as a representative example, 16 of the TOVS (Tiros-N Operational Vertical Sounder) infrared channels, namely the seven 15  $\mu\text{m}$  channels, the five 4.3  $\mu\text{m}$  channels, the three 6.3  $\mu\text{m}$  water vapor channels and the ozone channel at 9.6  $\mu\text{m}$ . For each of these spectral regions, Table 2 gives the total number of data points (sum over all the layers) computed by a classical line-by-line model on the basis of the frequency step mentioned above (column 2) and the corresponding number of data points effectively stored in the 4A data set per temperature sampled. In this example, the value of  $\epsilon$  is 0.005. If we assume, for the sake of simplicity, that the transmittance vectors stored in 4A are computed for 10 values of the temperature, which would correspond to a maximum range of variation of 50°C for each layer if the temperature sampling interval  $\Delta T$  is equal to 5°C, the numbers given in Table 2 must be multiplied by 10. It may easily be verified that such a volume of data is compatible with the capacity of standard magnetic direct access devices. In fact, the temperature range of 50°C is too large for some layers in the atmosphere and may be too small for others, for example, at ground level. The variations introduced in the number of temperatures sampled for each layer compensate one another. Similarly, as indicated above, the temperature sampling step  $\Delta T$  must be varied according to the spectral region and to the sensitivity of transmittances to temperature variations. For clear spectral regions, generally associated to lines with relatively high ground state energy values, this sensitivity is often high and  $\Delta T$  must eventually be reduced. Fortunately, such spectral regions correspond to small numbers of contributing points (transmittance is close to 1). For opaque spectral regions, it is almost the contrary since strong lines, in most cases, correspond to low ground state energy values and, then, to a relative insensitivity to temperature variations. This is also very fortunate since high-altitude layers correspond to large numbers of contributing points (see Table 1) and reducing  $\Delta T$  too much would have resulted in too big a volume of data.

Before being stored in the 4A data set, each transmittance value is transformed to its natural logarithm—the optical depth. Indeed, multiplying or exponentiating transmittances respectively correspond to adding or multiplying optical depths, which is simpler.

### 3. The 4A line-by-line transmittance computation method

We consider now an arbitrary atmosphere defined by its temperature and mixing-ratio profiles of the gases absorbing in the spectral region ( $\nu_a, \nu_b$ ). Com-

TABLE 2. Comparison between the number of data points computed by a classical line-by-line model and the number of data points effectively stored in the 4A data set ( $\epsilon = 0.005$ ).

Spectral region (cm <sup>-1</sup> )	Total number of data points computed ( $\times 10^{-9}$ )	Number of data points stored in the 4A data set ( $\times 10^{-6}$ )
650–780	4.20	0.51
990–1065	0.32	0.20
1170–1565	1.30	0.20
2160–2390	2.60	0.70

putation of transmittances between any two points in the atmosphere versus frequency in this spectral region, using the 4A data set, proceeds from the three following steps:

1) The atmosphere is first divided into  $N$  pressure levels according to the stratification used in the 4A data set; values of the temperature  $T_i$  and mixing ratio profiles  $q^g$ , the index  $g$  specifying one absorbing gas, are derived for each layer labeled by the index  $i$  (the index  $i$  varying from 1 to  $N-1$ ).

2) To each layer, from the value of the index  $i$ , directly related to pressure, and from the predetermined temperature, corresponds in the 4A data set, a set of vectors representing the optical depth of the layer (logarithm of transmittance) versus frequency: one for the sum of the gases with a constant mixing ratio and one for each of the gases whose mixing ratio varies with altitude. These vectors are immediately reached owing to an address simply obtained from the values of  $i, T_i$  (which is first transformed to the closest of the temperature sampled in the 4A for the layer  $i$ ) and  $g$ . Generally, these vectors present discontinuities in frequency (corresponding to discontinuities of the frequency-marker index) since points whose optical depth is too close to zero have not been stored. So as to ensure the continuity in frequency required for the derivation of the transmission function, these vectors must be completed by reinserting the missing points. We have chosen to give these missing points a constant value of the optical depth close to zero but different from zero, which, in a certain way, must be considered as the mean value of the optical depths which have not been stored. In the following, this value will be referred to as  $\epsilon'$ . One may notice that giving  $\epsilon'$  a nonzero value allows the missing points to effectively participate in subsequent computations (modifications of the reference values of the zenith angle and of the mixing ratios).

So transformed, each vector is multiplied by a constant determined for each layer i.e.,

$$p = (\sec\theta/\sec\theta_{\text{ref}})[q^g/(q^g)_{\text{ref}}], \quad (1)$$

where  $\theta$  is the true zenith angle and  $\theta_{\text{ref}}$  the ref-

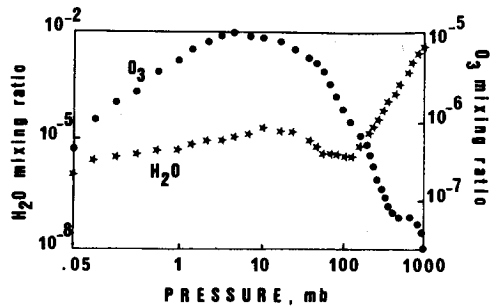


FIG. 2. The  $\text{H}_2\text{O}$  and  $\text{O}_3$  mixing ratio reference profiles of the Earth atmosphere, in the 4A model, versus logarithm of pressure.  $\text{H}_2\text{O}$  (scale on the left);  $\text{O}_3$  (scale on the right).

reference zenith angle used in constructing the 4A predetermined data set;  $q_i^g$  is the mixing ratio of the gas labeled by  $g$  at layer  $i$  and  $(q_i^g)_{\text{ref}}$  its reference value in the 4A. These vectors are then summed over the absorbing gases and exponentiated using a very fast procedure giving the transmittance of layer  $i$  versus frequency in the conditions of the atmosphere actually considered.

If we consider, as an example, the vertical sounding of an atmosphere from a satellite, transmittances computation proceeds from the highest ( $i = 1$ ) layer to the lower layers. Transmittances from the top to the  $i$ th layer are obtained by multiplying transmittances from the top and the  $(i - 1)$ th layer by those of the  $i$ th layer after a convenient interpolation for the vector with the largest frequency step. Results of this step are "monochromatic" transmittances versus frequency between the top and the stratification levels of the atmosphere. At each of these levels, in view of eventual subsequent radiance computations, the spectral resolution may be degraded and adapted to the frequency step necessary to a good representation of both the instrument response function and the blackbody function.

The rapidity of the 4A line-by-line method is mainly due to the fact that most of the long and tedious computations have been absorbed, once and for all, by the creation of the Automated Atmospheric Absorption Atlas. In the next sections, we present several applications of this method in connection with three different types of satellite experiments: the High-Resolution Infrared Sounder (HIRS/2) on TIROS-N, the infrared imagery on METEOSAT for the study of the atmosphere of Earth; and the Infrared Interferometer Spectrometer (IRIS) on VOYAGER for the study of the Jovian atmosphere.

#### 4. Application of the 4A line-by-line computation method to the High-Resolution Infrared Sounder (HIRS/2) on TIROS-N

The HIRS/2 instrument on TIROS-N has 20 channels among which we have, in a first step, more

particularly studied the seven channels at  $15 \mu\text{m}$ , the window at  $11 \mu\text{m}$ , the three water vapor channels around  $6.3 \mu\text{m}$  and the five channels at  $4.3 \mu\text{m}$ . Synthetic radiances (converted into radiometric brightness temperatures) obtained by using the line-by-line method based on the 4A predetermined data set have been compared to observed brightness temperatures acquired on 6, 9, and 10 July, 1979 and processed by the Centre de Météorologie Spatiale in Lannion (France). For these computations, the 4A data set has been designed on the basis of an atmosphere divided into 37 layers (38 pressure levels) between 1013.25 mb (actually, the ground pressure may be varied) and 0.05 mb. Each layer is given a maximum temperature variation of  $50^\circ\text{C}$  from  $(T_{\text{min}})_i$  to  $(T_{\text{min}})_i + 50^\circ\text{C}$  with a temperature sampling step  $\Delta T = 5^\circ\text{C}$ . The two extreme temperature profiles are shown on Fig. 1. The reference zenith angle is such that  $\sec\theta_{\text{ref}} = 1.1$  ( $\theta_{\text{ref}} \approx 25^\circ$ ). The water vapor and ozone reference mixing ratio profiles are shown in Fig. 2. The numbers  $\epsilon$  and  $\epsilon'$  have respectively been given the values 0.005 and 0.0005. These numerical values essentially proceed from experience with the 4A model and their choice is not unique since each of them is connected to the others. Let us examine this point in more detail.

The value of  $\epsilon$  directly controls the accuracy of transmittances resulting from the use of the 4A model:  $\epsilon = 0$  corresponds to the classical line-by-line method with its full accuracy (numerically greater than that of other atmospheric or spectroscopic parameters) and increasing  $\epsilon$  leads to keeping less and less data points in the 4A data set, which means decreasing the accuracy. In the same way, the larger the value of  $\theta_{\text{ref}}$  ( $\sec\theta_{\text{ref}} = 2$  at maximum for the HIRS/2 instrument) and of  $(q_i^g)_{\text{ref}}$ , the larger the optical depth. Consequently, for larger values of these two quantities, more data points are kept in the 4A data set than for smaller values, resulting in an increasing accuracy. After several tests with  $\epsilon$  (from  $\epsilon = 0.999$  to  $\epsilon = 0.95$ ), for different values of  $\theta_{\text{ref}}$  and for the reference mixing ratio profiles of Fig. 2, we have chosen to give  $\epsilon$  a value relatively small (0.005) which is able to adjust the numerical accuracy of the model to a value slightly greater than that which is required on a pure physical point of view. Another solution could consist in increasing  $\epsilon$  while increasing  $\theta_{\text{ref}}$  and  $(q_i^g)_{\text{ref}}$  at the same time. The last parameter  $\epsilon'$  is chosen on a pure "experimental" basis; experience with the 4A model has shown that  $\epsilon' = 0$  leads to transmittances slightly too large (atmosphere slightly too transparent) as compared to a classical line-by-line model. The value we have adopted ( $\epsilon' = 0.0005$ ), jointly with those of  $\epsilon$ ,  $\theta_{\text{ref}}$  and  $(q_i^g)_{\text{ref}}$ , gives perfect agreement with that type of computation in the sense that the difference between the 4A model and the

classical line-by-line model is less than the noise of the HIRS/2 instrument. Moreover, introducing this parameter with a value close to but different from zero has proven essential when changing the values of the zenith angle and the mixing ratios from reference values to larger values.

Since the results of the classical line-by-line computations, which are at the basis of the 4A pre-determined data set, are kept monochromatically, the values of  $\epsilon$ ,  $\theta_{ref}$  and  $(q_g^i)_{ref}$  may be simply and rapidly changed by reprocessing these results on the basis of the new values. The result is a new 4A data set corresponding to these new values. The 4A data set is not affected by a modification of the value of  $\epsilon'$ . The standard line-by-line procedure from which the 4A data set is constructed has been described by Scott (1974) and Chedin *et al.* (1978). Wings of the lines are explored up to  $1200\alpha$ ,  $\alpha$  being the line half-width. Two types of continuum are taken into account—the water vapor continuum as proposed by Roberts *et al.* (1976) and the nitrogen continuum formulated by Susskind and Searl (1977). Ozone absorption in the  $15 \mu\text{m}$  spectral region is computed from the weak line approximation. For the three days mentioned above, a set of 28 matched HIRS/2 observations over apparently cloud free oceanic areas and radiosonde observations at noon were collected, and aligned within three hours in time. This data set permits us to make an initial evaluation of the quality of the 4A model although it is not large enough and no information is available on the temperature of the upper atmosphere (no rocketsonde observations).

Limitations of information concerning the upper levels of the atmosphere are shown in Table 3 where for each of the 28 HIRS-2 observations on 6, 9, and 10 July 1979 we show the highest levels (mb) of the atmosphere where radiosonde temperatures and dew points were available. Due to this lack of information we have been led to reduce the number of significant comparisons in the more absorbing channels, and to extend the dew-point and temperature profiles by standard profiles to the top of the atmosphere.

Results of these comparisons are shown in Figs. 3a–3n and in Table 4. Channels 1, 9 (ozone channel) and 17 are not presented. The signal-to-noise ratio of channel 1 was too small and, as indicated above, the information available on the upper atmosphere for all channels was poor. In addition short-wave channels could possibly be affected by scattering and fluorescence in sunlight. Table 4 presents, for the 14 channels considered, the results of a simple statistical analysis of the deviations between calculated and observed brightness temperatures. As an indication, these results have been compared to similar results obtained by Abel *et al.* (1978)<sup>1</sup> for the HIRS experiment on board Nimbus 6

TABLE 3. Description of the radiosonde data associated with the TIROS-N HIRS/2 experiment on 6, 9, and 10 July 1979. Columns A, B, C give the name of the station, its latitude and longitude. In each of the columns D, E, F, respectively corresponding to 6, 9 and 10 July, are given the highest levels of the atmosphere (mb) for which the temperature (columns a) and the dew point (columns b) were available from radiosonde data.

A	B	C	D		E		F	
			a	b	a	b	a	b
Ajaccio	41.91	8.80			43	275	46	287
Bordeaux	44.83	359.30	11	310	23	278	29	303
Brest	48.45	355.59	20	313			40	311
Cagliari	39.25	9.05			150	400		
Camborne	50.21	354.69	106	316	100	236		
Casablanca	33.56	352.34	32	268			120	300
dar el Beida	36.71	3.25			128	264	70	262
De Bilt	52.10	5.18					38	400
Gibraltar	36.15	354.67	20	287	20	267		
la Corogne	43.36	351.59	13	654	41	600		
Lisbonne	38.76	350.87	170	365	233	400		
R	47	343	20	300	37	282	16	304
M	66	2			17	326		
Shanwell	56.43	357.14					28	357
Stavanger	58.86	5.66			16	400	26	382

using their very fast empirical model for atmospheric transmittance function computation. However, one must keep in mind that this comparison concerns two different instruments and that HIRS/1 is slightly less accurate than HIRS/2.

Several features are noteworthy: the agreement in the temperature channels ( $15$  and  $4.3 \mu\text{m}$  spectral regions) is generally satisfactory but is degraded for channels sounding the upper atmosphere. This is due to the lack of rocketsonde observations. Channel 8 (window) is affected by a relatively poor knowledge of sea surface temperature. Channel 10, for water vapor sounding near the surface ( $\sim 900$  mb), is remarkably good. Channels 11 and 12 for water vapor sounding at higher levels are affected by the lack of knowledge of the  $\text{H}_2\text{O}$  mixing ratio above 300 mb. Systematic deviations of a relatively large amplitude (up to 2.3 K) are observed for channels 5, 6, 10, 14 and 15. They can be simply corrected empirically. It is our feeling that they come, to a large extent, from an insufficient knowledge of the line absorption in the far wings and, thus, from discrepancies between synthetic and true transmittances. In this respect it may be noticed that the largest systematic deviations in the  $15 \mu\text{m}$  region are for channels 5 and 6 where calculated values are smaller than observed values, contrary to what was found by several authors.<sup>2</sup> Comparisons

<sup>2</sup> Spänkuch, D., W. Döhler, U. Feister, and J. Güldner, 1980: Results of the Fourier spectrometer missions obtained in the GDR. Presented at the International Radiation Symposium, Fort Collins, CO, Radiation Commission of the Int. Assoc. Meteor. Atmos. Phys. (IAMAP).

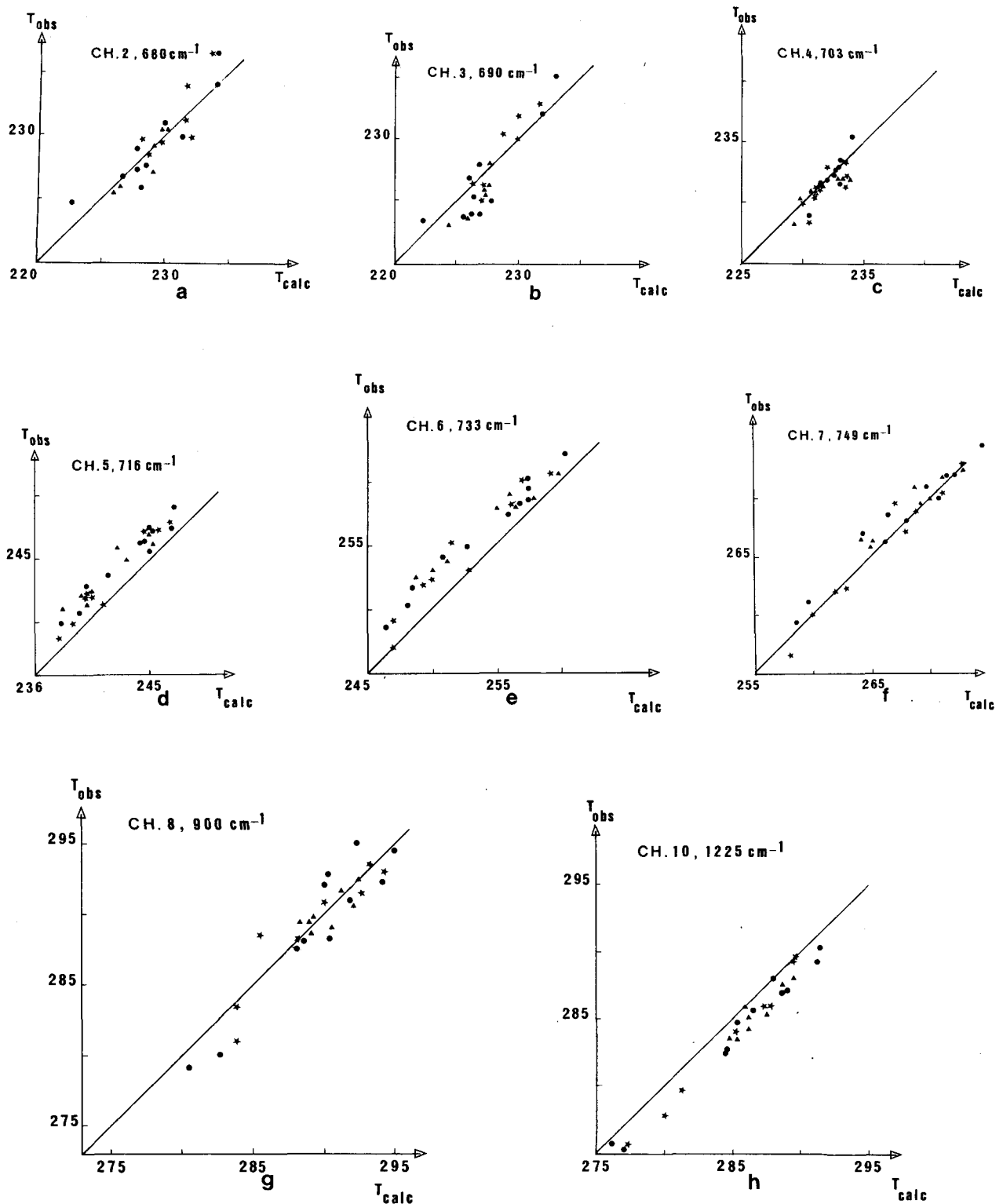


FIG. 3. TIROS-N-HIRS/2 experiment. Observed equivalent temperatures (y axis) versus the 4A computed equivalent temperatures (x axis): (a)–(f), channels 2–7 of the 15  $\mu m$  spectral region; (g), channel 8, 10  $\mu m$  window; (h)–(j), channels 10–12 of the 6.3  $\mu m$  spectral region; (k)–(n), channels 13–16 of the 4.3  $\mu m$  spectral region. The central wavenumber of each channel is given at the top of each figure.

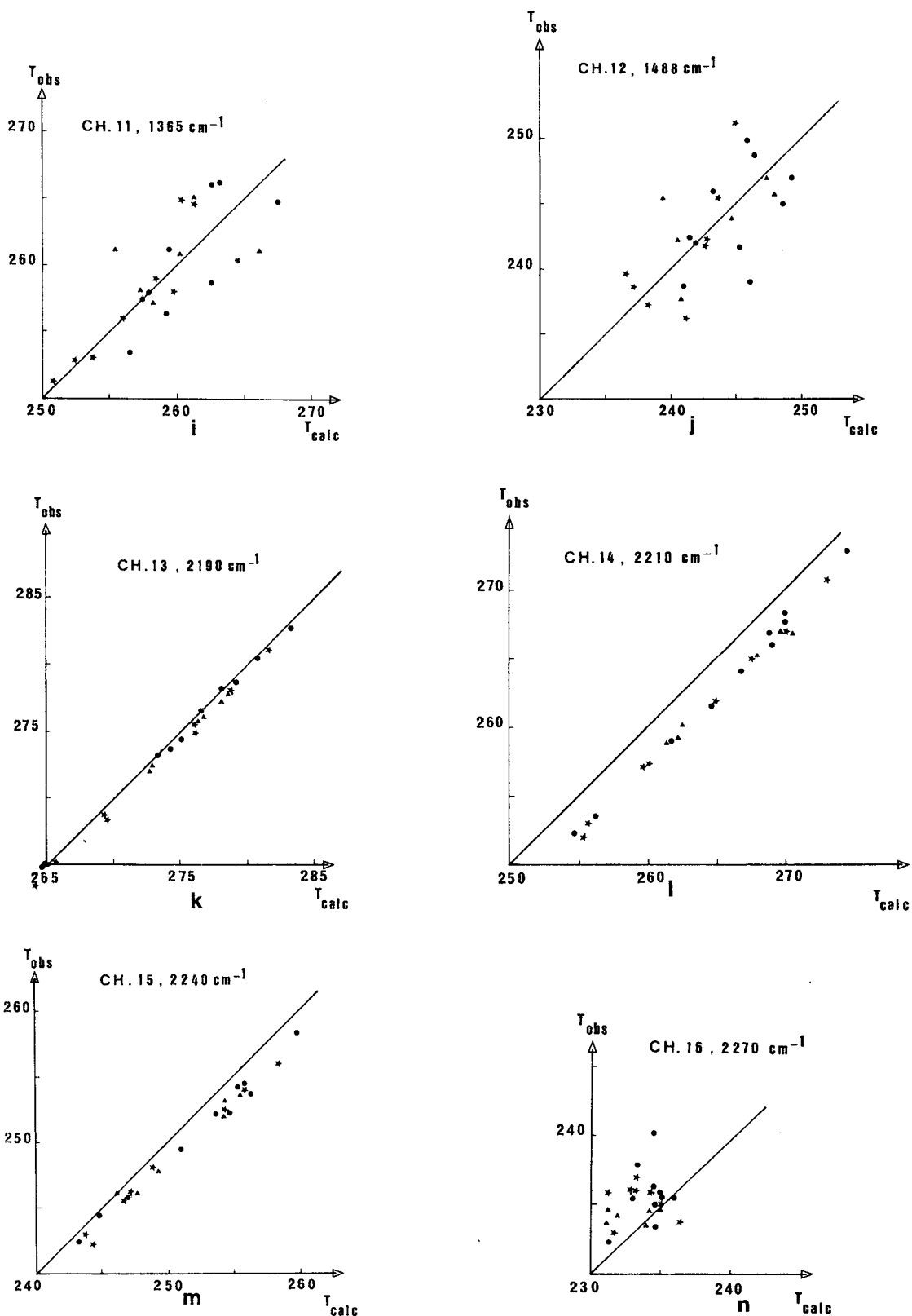


FIG. 3. (Continued)



TABLE 4. Comparisons between 4A computed and observed clear-column equivalent temperatures for 14 channels of the TIROS-N HIRS/2 experiment of July 1979.

	Channel number													
	2	3	4	5	6	7	8	10	11	12	13	14	15	16
$\omega_0$ (cm <sup>-1</sup> )	680	690	703	716	733	749	900	1225	1365	1488	2190	2210	2240	2270
Number of samples	23	23	26	28	28	28	27	28	24	24	24	24	24	24
Mean deviation (K) (calc - obs)	-0.1	0.4	0.4	-1.9	-2.2	-0.6	0.2	1.5	0.0	-0.3	0.7	2.7	1.4	-1.7
Standard deviation, (K)*	1.5 (1.8)	1.6 (1.6)	1.0 (1.3)	0.7 (1.4)	0.9 (1.8)	1.1 (2.5)	1.6 (4.3)	0.6 (3.3)	2.9 —	3.4 (5.6)	0.5 (2.8)	0.5 (1.8)	0.7 (0.9)	1.9 (1.7)

\* Parenthesized numbers are from Abel *et al.* (see footnote 1) and concern the HIRS/1 instrument on Nimbus 6.

between the results obtained by using the 4A model and observations are still in progress with more numerous and reliable radiosoundings. These comparisons will allow us to refine the above preliminary conclusions.

Table 5 gives the computation times obtained with the 4A transmittance model for four spectral regions of the HIRS/2 instrument, representing 16 channels. The number of channels included in the computation is given in column 2 for each spectral region. These spectral intervals are relatively wide and are divided into subintervals as explained in Section 2. The number of such subintervals is given in column 3. Computation times are given in column 4 in seconds for the AMDAHL-V7 computer which is, for the present type of computation, about 1.7 times faster than the IBM 370/168. These numbers are 20–40 times smaller than those using a standard line-by-line method.

## 5. Other applications of the 4A line-by-line model

### a. METEOSAT infrared channels

Calibration of the METEOSAT infrared channels (water vapor and window channels) is still under discussion and no probing comparisons can be made between observed and calculated radiances. Using the standard line-by-line transmittance model developed by Scott (1974), Poc *et al.* (1980) have performed a series of computations concerning the water vapor METEOSAT channel. Under exactly the same conditions, we have made the same com-

putations using the new 4A transmittance and radiance model and have obtained essentially perfect agreement (to within 0.5%) between the numbers provided by a standard line-by-line model and the 4A model. Thus, the effect of replacing transmittances too close to 1 by a constant  $(1 - \epsilon')$  is negligible. A number of similar comparisons have been carried out in other spectral regions (15  $\mu\text{m}$ , window, etc . . .) with the same conclusion. The computation times obtained for the water vapor channel (1342–1774 cm<sup>-1</sup>) and for the window channel (760–940 cm<sup>-1</sup>) are 30 s and 3 s, respectively with the AMDAHL-V7 computer [ or equivalently, 0.7 s (10 cm)<sup>-1</sup>, and 0.15 s (10 cm)<sup>-1</sup>].

### b. Simulation of a high-resolution balloon experiment

The 4A line-by-line transmittance and radiance computation method is general and may be applied to any kind of atmospheric experiment. As an example of this generality, we have computed, using the 4A data set, a synthetic spectrum of the atmosphere as it could be recorded by a balloonborne instrument looking at the sun, having a mean spectral resolution of 0.7 cm<sup>-1</sup>. This synthetic spectrum, shown in Fig. 4, required a total computation time of 30 s (AMDAHL-V7).

### c. The Infrared Interferometer Spectrometer (IRIS) on VOYAGER

The VOYAGER IRIS data on the Jovian atmosphere provide significant advantages over previous measurements. A large number of well-calibrated spectra were obtained from various locations on the disk of Jupiter with a relatively high spectral resolution. For the first time spectra were measured from 4 to 55  $\mu\text{m}$ , providing simultaneous information on the atmosphere of this planet from the 0.1 mb pressure level up to several bars and allowing uncertainties due to temporal and spatial variations of the atmosphere to be eliminated. The recorded IRIS spectra are made of two parts: 6.5–55  $\mu\text{m}$

(Footnote 2 continued)

McClatchey, R. A., 1980: An atmospheric temperature profile measured with an *in situ* infrared radiometer. Presented at the International Radiation Symposium, Fort Collins, CO.

Neuendorffer, A. C., 1980: Satellite IR radiance deficits and transmittances. To be presented at the Topical Meeting on Spectroscopy in Support of Atmospheric Measurements, Sarasota, FL. Opt. Soc. Amer.

Weinreb, M. R., 1979: Atmospheric transmission for remote temperature sounding. Soc. Photo. Opt. Instrum. Engrs., 195, 20–30.

TABLE 5. Computation times achieved with the 4A model in four spectral regions.

Spectral range	Number of HIRS/2 channels	Number of subintervals	Computation time (*) for one meteorological situation (s)	Computation time (*) per 10 cm <sup>-1</sup> (s)
15 μm 655–780 cm <sup>-1</sup>	7	25 (5 cm <sup>-1</sup> each)	34	0.27
11 μm 860–940 cm <sup>-1</sup>	1	14 (15 cm <sup>-1</sup> each)	7	0.03
6.3 μm 1169–1565 cm <sup>-1</sup>	3	18 (22 cm <sup>-1</sup> each)	28	0.07
4.3 μm 2160–2390 cm <sup>-1</sup>	5	9 (25 cm <sup>-1</sup> each)	34	0.15

\* Obtained on the AMDAHL-V7 of the Centre Inter-Régional de Calcul Electronique (CIRCE) of the C.N.R.S. at Orsay (France). Computations of convoluted transmittances, weighting functions, radiances, brightness temperatures and input/output operations are included.

(180–1500 cm<sup>-1</sup>) where emission comes from the stratosphere and the upper troposphere and the 5 μm window (1700–2400 cm<sup>-1</sup>) where emission comes from the lower troposphere. The most important absorption phenomena in these spectral regions are due to the hydrogen-helium continuum, ammonia, methane (CH<sub>4</sub> and CH<sub>3</sub>D), phosphine, water vapor, etc. . . . The far-infrared spectral region (180–310 cm<sup>-1</sup>) is dominated by ammonia opacity and the medium-infrared spectral region (800–1520 cm<sup>-1</sup>) is dominated by methane, ammonia and phosphine opacities. The H<sub>2</sub>/He continuum takes place between these two regions as shown in Fig. 5 which represents a typical experimental IRIS spectrum of the Jovian atmosphere (from Hanel *et al.*, 1979). New or more accurate line parameters were taken: for CH<sub>4</sub>, from Chedin *et al.* (1978); for NH<sub>3</sub>, from Husson *et al.*<sup>3</sup>; for CH<sub>3</sub>D, from Tarrago *et al.* (1980) and Pinkley *et al.* (1977); for PH<sub>3</sub>, from Yin and Rao (1974); for the H<sub>2</sub>/He

continuum, from Birnbaum and Cohen (1976) and Birnbaum (1978).

This spectroscopic line parameter compilation has been merged in our general spectroscopic data compilation GEISA [Gestion et Étude des Informations Spectroscopiques Atmosphériques (Chedin *et al.*, 1980)<sup>4</sup>].

The 4A data set for the Jovian atmosphere has been constructed using the standard line-by-line model described by Scott (1974) with line wing exploration up to 1200α (α being the line half-width). The atmosphere is divided into 50 layers (51 pressure levels) ranging from 3000 to 0.05 mb. Each layer is given a maximum temperature variation of 35°C with a temperature sampling step ΔT = 5°C. These numbers have been chosen on the basis of preliminary results supplied by the VOYAGER mission. The reference zenith angle, ε and ε' have the same values as for the Earth 4A data set (see Section 4). Retrievals of atmospheric temperature and mixing ratios profiles from the IRIS spectra have been recently carried out (Kunde *et al.*, 1980). Using these retrieved profiles and the Jovian 4A data set described above we have computed synthetic spectra covering the two spectral regions 180–310 cm<sup>-1</sup> and 750–1520 cm<sup>-1</sup>. For the first region, the computation time was 5 s with the 4A line-by-line method and 179 s with our classical line-

<sup>3</sup> Husson, N., A. Chedin and N. A. Scott, 1979: Paramètres spectroscopiques de la molécule d'ammoniac dans la région 32–7.5 μm. Internal Report LMD No. 90, Paris, France [paper in preparation].

<sup>4</sup> Chedin, A., N. Husson, N. A. Scott and I. Cohen, 1980: Gestion et étude des informations spectroscopiques atmosphériques. Internal Report LMD No. 108.

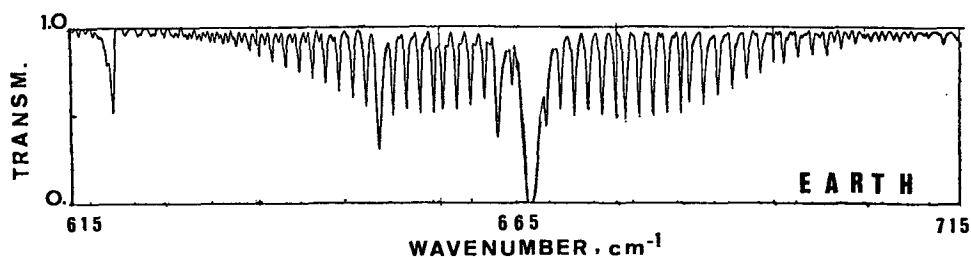


FIG. 4. A simulated balloonborne experiment looking at the sun with a mean resolution of 0.7 cm<sup>-1</sup> in the 15 μm spectral region. The mean computation time is equal to 0.3 s (10 cm<sup>-1</sup>).

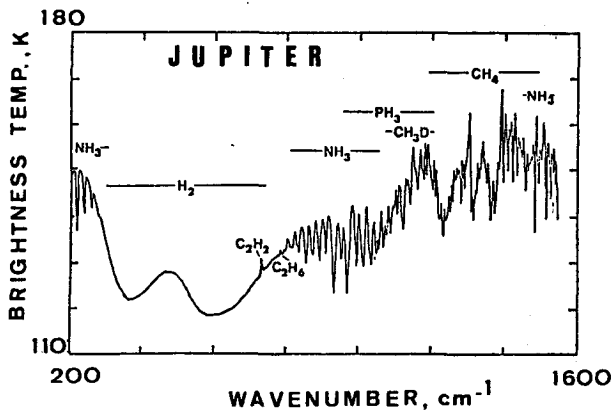


FIG. 5. A typical spectrum of the atmosphere of Jupiter as registered by the IRIS instrument on Voyager. The mean computation time for the restitution of such a spectrum in these spectral limits with the 4A model is equal to 0.7 s  $(10 \text{ cm}^{-1})^{-1}$  for a 50-layer model.

by-line model. For the second region, these two computation times were 98 s and 2470 s, respectively. No significant differences have been observed between the two kinds of computations.

#### 6. Additional remarks: Storing the Automated Atmospheric Absorption Atlas

As a result of the uncertainties in the spectroscopic line parameters and in the meteorological parameters, three digits are enough (if not more than enough) to represent atmospheric transmittance in the great majority of the cases. Consequently, this quantity ranges from 0.001 for the smallest value (in fact, considered as being zero) to  $1 - \epsilon$  (e.g., 0.999 if  $\epsilon = 0.001$ ). Its natural logarithm, changed in sign and multiplied by 1000, may be measured by an integer number ranging from 6908 to 1 (case where  $\epsilon = 0.001$ ). It is under that form that transmittances resulting from the standard line-by-line computations are stored, together with an index representing the frequency, to form the 4A data set.

**Acknowledgments.** Many thanks are due to the Centre de Météorologie Spatiale de Lannion, France, and particularly to Guy Rochard, for making the TIROS-N observations available to us. We are deeply grateful to Nicolas Bériot for collecting and critically examining the radiosonde data, for designing the navigation program of the TIROS-N observations and for choosing the 28 matchups. We have benefitted from helpful discussions with Daniel Gautier, member of the VOYAGER team, about the modeling of the Jovian atmosphere. We are greatly indebted to Pr. André Berroir for his careful read-

ing of the manuscript and his suggestions for improvements in the text.

*Note added in proof:* Since the final form of this manuscript, this work has been carried on in three directions: 39 layers instead of 37 (see Fig. 1) are now used for the representation of the temperature and pressure profiles. The value of  $\epsilon'$  is now tuned to the mean value of the optical depth of non-stored points in each layer (see Section 3). Due to refinements of the direct access procedures for input/output operations, computation times have been reduced by a factor of 1.3 with respect to the computation times given in Table 5.

#### REFERENCES

- Birnbaum, G., 1978: Far-infrared absorption in the  $\text{H}_2$ - $\text{H}_2$  and  $\text{H}_2$ -He mixtures. *J. Quant. Spectrosc. Radiat. Transfer*, **19**, 51-62.
- , and E. R. Cohen, 1976: Theory of line shape in pressure induced absorption. *Can. J. Phys.*, **54**, 593-602.
- Chedin, A., N. Husson, N. A. Scott and D. Gautier, 1978:  $\nu_4$  band of methane ( $^{12}\text{CH}_4$  and  $^{13}\text{CH}_4$ ). Line parameters and evaluation of Jovian atmospheric transmission at 7.7  $\mu\text{m}$ . *J. Mol. Spectrosc.*, **71**, 343-368.
- Fleming, H. E., and L. M. McMillin, 1977: Atmospheric transmittance of an absorbing gas: a computationally fast and accurate transmittance model for slant paths at different zenith angles. *Appl. Opt.*, **16**, 1366-1370.
- Hanel, P., B. Conrath, M. Flasar, L. Herath, V. Kunde, P. Lowman, W. Maguire, J. Pearl, P. Pirraglia, R. Samuelson, D. Gautier, L. Horn, S. Kumar and C. Ponnampuram, 1979: Infrared observations of the Jovian system from Voyager-2. *Science*, **206**, 952-956.
- Kunde, V., R. Hanel, L. Herath, W. Maguire, D. Gautier, J. P. Balluteau, A. Marten, A. Chedin, N. Husson and N. A. Scott, 1980: The lower atmosphere composition of Jupiter's North equatorial belt from the Voyager infrared investigation. Submitted to *J. Geophys. Res.*
- McMillin, L. M., and H. E. Fleming, 1976: Atmospheric transmittance of an absorbing gas: a computationally fast and accurate transmittance model for absorbing gases with constant mixing ratios in inhomogeneous atmosphere. *Appl. Opt.*, **15**, 358-363.
- , H. E. Fleming and M. L. Hill, 1979: Atmospheric transmittance of an absorbing gas: a computationally fast and accurate transmittance model for absorbing gases with variable mixing ratios. *Appl. Opt.*, **18**, 1600-1606.
- Pinkley, L. W., K. Narahari Rao, G. Tarrago, G. Poussiguet and M. Dang-Nhu, 1977: Analysis of the  $\nu_6$  band of  $^{12}\text{CH}_4$  at 8.6  $\mu\text{m}$ . *J. Mol. Spectrosc.*, **68**, 195-222.
- Poc, M. M., M. Roulleau, N. A. Scott and A. Chedin, 1980: Quantitative studies of METEOSAT water vapor channel data. *J. Appl. Meteor.*, **19**, 868-876.
- Roberts, R. E., J. E. A. Selby and L. M. Biberman, 1976: Infrared continuum absorption by atmospheric water vapor in the 8-12  $\mu\text{m}$  window. *Appl. Opt.*, **14**, 2085-2090.
- Scott, N. A., 1974: A direct method of computation of the transmission function of an inhomogeneous gaseous medium. *J. Quant. Spectrosc. Radiat. Transfer*, **14**, 691-704.
- Susskind, J., and J. E. Searl, 1977: Atmospheric absorption near 2400  $\text{cm}^{-1}$ . *J. Quant. Spectrosc. Radiat. Transfer*, **18**, 581-587.
- Tarrago, G., K. Narahari Rao and L. W. Pinkley, 1980: Analysis of the  $\nu_3$  band of  $^{12}\text{CH}_3\text{D}$  at 7.6  $\mu\text{m}$ . *J. Mol. Spectrosc.*, **79**, 31-46.
- Yin, P. K. L., and K. Narahari Rao, 1974:  $\nu_2$  and  $\nu_4$  fundamentals of phosphine occurring at 8-12  $\mu\text{m}$ . *J. Mol. Spectrosc.*, **15**, 199-207.